

# Characterization of MCM-48 Silicas with Tailored Pore Sizes Synthesized via a Highly Efficient Procedure

Michal Kruk and Mietek Jaroniec\*

Department of Chemistry, Kent State University, Kent, Ohio 44242

Ryong Ryoo and Sang Hoon Joo

Department of Chemistry and School of Molecular Science (BK21), Korea Advanced Institute of Science and Technology, Taeduk Science Town, Taejeon, 305-701 Korea

Received December 7, 1999. Revised Manuscript Received March 6, 2000

MCM-48 silicas have been prepared via a high-yield synthesis procedure using mixtures of cationic alkyltrimethylammonium surfactants (alkyl chain length from 12 to 20 carbon atoms) and neutral cosurfactants. This is the first reported successful synthesis of MCM-48 using eicosyltrimethylammonium surfactant. The samples, especially those synthesized using cationic surfactants with cetyl, octyl, and eicosyl chains, were found to exhibit a high degree of structural ordering, which manifested itself in very well-resolved X-ray diffraction (XRD) patterns, and remarkably narrow capillary condensation steps after the template removal. The latter could be achieved not only via calcination, but also via ethanol/HCl washing. The unit-cell size and pore size of MCM-48 were found to be determined by the alkyl chain length of the cationic surfactant used. The calcined MCM-48 samples had BET specific surface areas of about  $1100 \text{ m}^2 \text{ g}^{-1}$ , large primary mesopore volumes (up to  $1.15 \text{ cm}^3 \text{ g}^{-1}$ ), XRD  $d_{211}$  interplanar spacings from 3.6 to 4.5 nm, and average primary mesopore sizes covering the range from 3.5 up to as large as 4.5 nm. The percentage of template in the as-synthesized MCM-48 samples assessed using thermogravimetry (TGA) was found to be correlated with the primary mesopore volume of the calcined materials. The as-synthesized MCM-48 had inaccessible primary mesoporosity and its external surface exhibited relatively weak interactions with nitrogen adsorbate, similar to alkylsilyl-modified silicas and contrary to bare silicas. This indicated that the external surface was covered with surfactant ions attached to the silicate framework, as previously demonstrated for MCM-41. The differences between nitrogen interactions with surfactant–silicate and silica surfaces provided a possibility for detecting the residual surfactant left after the ethanol/HCl washing using nitrogen adsorption.

## Introduction

MCM-48 silica,<sup>1</sup> whose mesoporous structure consists of an enantiomeric pair of separate three-dimensional channel systems,<sup>2</sup> has recently attracted much attention as a prospective catalyst, adsorbent, and template for the synthesis of nanostructures. Studies of synthesis, modification, characterization, and application of MCM-48 were recently reviewed,<sup>3–5</sup> but since then, remarkable progress has been made in the following areas: An approach for high-yield synthesis of pure-silica MCM-48<sup>6</sup> and a new method for preparation of spherical

MCM-48 particles<sup>7</sup> were reported. Incorporation of MCM-48 framework with various heteroatoms, such as Al, Cu, Zn, Cr, Mn, Mo, Zr, and Ti, was further explored.<sup>8–14</sup> Formation of nanosized platinum clusters<sup>15</sup> and  $\text{Fe}_2\text{O}_3$  nanoparticles<sup>16</sup> within the MCM-48 framework as well as formation of metal complexes by

\* Corresponding author: Telephone: (330) 672 3790. Fax: (330) 672 3816. E-mail: jaroniec@columbo.kent.edu.

(1) Beck, J. S.; Vartuli, J. C.; Roth, W. J.; Leonowicz, M. E.; Kresge, C. T.; Schmitt, K. D.; Chu, C. T.-W.; Olson, D. H.; Sheppard, E. W.; McCullen, S. B.; Higgins, J. B.; Schlenker, J. L. *J. Am. Chem. Soc.* **1992**, *114*, 10834.

(2) Monnier, A.; Schuth, F.; Huo, Q.; Kumar, D.; Margolese, D.; Maxwell, R. S.; Stucky, G. D.; Krishnamurty, M.; Petroff, P.; Firouzi, A.; Janicke, M.; Chmelka, B. F. *Science* **1993**, *261*, 1299.

(3) Morey, M. S.; Davidson, A.; Stucky, G. D. *J. Porous Mater.* **1998**, *5*, 195.

(4) Moller, K.; Bein, T. *Chem. Mater.* **1998**, *10*, 2950.

(5) Kruk, M.; Jaroniec, M.; Ryoo, R.; Kim, J. M. *Chem. Mater.* **1999**, *11*, 2568.

(6) Ryoo, R.; Joo, S. H.; Kim, J. M. *J. Phys. Chem. B* **1999**, *103*, 7435.

(7) Schumacher, K.; du Fresne von Hohenesche, C.; Unger, K. K.; Ulrich, R.; Du Chesne, A.; Wiesner, U.; Spiess, H. W. *Adv. Mater.* **1999**, *11*, 1194.

(8) Oye, G.; Sjoblom, J.; Stocker, M. *Microporous Mesoporous Mater.* **1999**, *27*, 171.

(9) Hartmann, M.; Racouchot, S.; Bischof, C. *Microporous Mesoporous Mater.* **1999**, *27*, 309.

(10) Cai, Q.; Wei, C. P.; Xu, Y. Y.; Pang, W. Q.; Zhen, K. J. *Chem. J. Chinese Univ.* **1999**, *20*, 344.

(11) Morey, M. S.; Stucky, G. D.; Schwarz, S.; Froba, M. *J. Phys. Chem. B* **1999**, *103*, 2037.

(12) Chen, F.; Song, F.; Li, Q. *Microporous Mesoporous Mater.* **1999**, *29*, 305.

(13) Xu, J.; Luan, Z.; Hartmann, M.; Kevan, L. *Chem. Mater.* **1999**, *11*, 2928.

(14) Ahn, W. S.; Lee, D. H.; Kim, T. J.; Kim, J. H.; Seo, G.; Ryoo, R. *Appl. Catal. A: General* **1999**, *181*, 39.

(15) Chatterjee, M.; Iwasaki, T.; Onodera, Y.; Nagase, T. *Catal. Lett.* **1999**, *61*, 199.

organosilane-functionalized MCM-48<sup>17</sup> were studied and procedures for improvement of the structural ordering<sup>18</sup> and hydrothermal stability of MCM-48<sup>6</sup> were proposed. Studies in the direction of pore size estimation,<sup>19</sup> assessment of mechanical stability,<sup>20</sup> and characterization of silica-heteroatom framework structure<sup>21</sup> were carried out. The MCM-48 structure was resolved using the single-crystal electron diffraction,<sup>22</sup> confirming the previous structural identification.<sup>2</sup> Consistent with these studies, nitrogen adsorption showed<sup>5</sup> that MCM-48 did not have any detectable microporosity and exhibited different pore volume/surface area ratio from that for MCM-41 silica<sup>1</sup> with nonintersecting and approximately cylindrical pores. In addition to these advances in synthesis, modification, and characterization, remarkable new applications of MCM-48 emerged. Ryoo and co-workers<sup>23</sup> reported the first successful synthesis of ordered mesoporous carbons using MCM-48 as a template. Similar synthesis was later reported by others, who also demonstrated that thus prepared ordered mesoporous carbons were promising electrochemical double-layer capacitors.<sup>24</sup> Moreover, organosilane-modified MCM-48 was found to be suitable as a packing for chiral HPLC separations.<sup>25</sup>

Since MCM-48 emerges as a promising catalyst, support for functional moieties and template for synthesis of advanced nanomaterials, it is important to identify procedures suitable for a cost-efficient synthesis of well-ordered contamination-free MCM-48 with a wide range of pore sizes and unit cell parameters. From this point of view, synthesis procedures based on mixed cationic–anionic<sup>12</sup> and cationic–neutral<sup>6,26</sup> surfactants are highly promising. A recently reported synthesis of MCM-48 using cationic alkyltrimethylammonium surfactants ( $C_nTMA^+$ ) and neutral cosurfactants (usually oligomeric ethylene oxide surfactants)<sup>6</sup> is particularly interesting, since it was found to be well-reproducible and provided remarkably high yields of the MCM-48 silica per mole of the template used. Moreover, the obtained materials exhibited a wide range of unit-cell sizes tailored by the chain length of the cationic surfactant used. In the current study, MCM-48 silicas templated by  $C_nTMA^+$ /cosurfactant mixtures were synthesized using the aforementioned procedure and its extension for  $C_{20}TMA^+$ , which is reported herein. The obtained samples were characterized by X-ray diffraction (XRD), nitrogen adsorption, and thermogravimetry (TGA), with emphasis on characterization of porous structures of calcined samples. Properties of as-synthe-

sized samples are compared to those of ethanol/HCl washed and calcined samples, and relations between these properties are discussed.

## Materials and Methods

**Materials.** The synthesis of MCM-48 using  $C_nTMA^+$ /cosurfactant mixtures was described in detail elsewhere.<sup>6</sup>  $C_nTMA^+$ :cosurfactant molar ratios were the following:  $C_{12}TMA^+$ :LE-3 = 0.75:0.25;  $C_{14}TMA^+$ :LE-4 = 0.8:0.2;  $C_{16}TMA^+$ :LE-4 = 0.85:0.15; and  $C_{18}TMA^+$ :Triton X-100 = 0.92:0.08, where LE-3, LE-4, and Triton X-100 denote  $C_{12}H_{25}O(C_2H_4O)_3H$ ,  $C_{12}H_{25}O(C_2H_4O)_4H$ , and  $CH_3C(CH_3)_2CH_2C(CH_3)_2C_6H_4O(C_2H_4O)_{10}H$ , respectively. The synthesis of eicosyltrimethylammonium-templated MCM-48 ( $n = 20$ ) was similar to that described in ref 6 and involved the starting molar composition of 5  $SiO_2$ : 1.25  $Na_2O$ :0.92  $C_{20}TMABr$ :0.08 Triton X-100:300  $H_2O$ . The surfactant solution and the silica source were rapidly mixed by vigorous shaking for 30 min at 323 K. Subsequently, the resulting synthesis gel was heated for 43 h at 373 K, cooled to 323 K, its pH was adjusted to 10 at 323 K by adding acetic acid, and finally the gel was heated for 48 h at 373 K before the product filtration. Other details of the synthesis procedure used can be found elsewhere.<sup>6</sup> As-synthesized (uncalcined, water-washed), ethanol/HCl washed, and calcined MCM-48 samples will in general be denoted as MCM-48-U, MCM-48-EA, and MCM-48-C. The particular as-synthesized, ethanol/HCl washed, and calcined MCM-48 samples will be referred to as Cn-U, Cn-EA, and Cn-C.

**Measurements.** Powder X-ray diffraction patterns were recorded on a Rigaku D/MAX-III diffractometer using  $Cu K\alpha$  radiation. Nitrogen adsorption isotherms were measured at 77 K on a Micromeritics ASAP 2010 volumetric adsorption analyzer. Before the measurements, MCM-48-C and -EA samples were outgassed under vacuum for 2 h at 473 K in the degas port of the adsorption apparatus. MCM-48-U samples were outgassed under vacuum at room temperature until the residual pressure dropped to 6 (or less)  $\mu mHg$ , which usually took several hours. Weight change curves were recorded under flowing nitrogen on a TA Instruments TGA 2950 high-resolution thermogravimetric analyzer using the high-resolution mode with maximum heating rate of 5  $K min^{-1}$ .

**Calculations.** The BET specific surface area<sup>27</sup> was calculated using data in a relative pressure range from 0.04 to 0.2. The total pore volume<sup>27</sup> was determined from the amount adsorbed at a relative pressure of about 0.99. The external surface area and primary mesopore volume for MCM-48-C and -EA samples were calculated using the  $\alpha_s$  plot method<sup>27,28</sup> with the silica reference nitrogen adsorption isotherm reported recently.<sup>29</sup> The calculations were carried out in the  $\alpha_s$  ranges 1.5–2.1 for C20-C and -EA; 1.5–1.9 for C18-C and -EA; and 1.3–1.8 for C14-EA and 1.3–1.7 for the other samples. The silica reference adsorption isotherm and the reference adsorption isotherm for octyldimethylsilyl-modified silicas<sup>30</sup> were used to examine the surface properties of the samples under study. The pore size distribution was calculated from adsorption branches of nitrogen isotherms using the Barrett–Joyner–Halenda<sup>31</sup> method with the statistical film thickness curve and the relation between the pore size and capillary condensation pressure determined using the Kruk–Jaroniec–Sayari (KJS) approach.<sup>32</sup>

(16) Froba, M.; Kohn, R.; Bouffaud, G.; Richard, O.; van Tendeloo, G. *Chem. Mater.* **1999**, *11*, 2858.

(17) Park, D. H.; Park, S. S.; Choe, S. J. *Bull. Korean Chem. Soc.* **1999**, *20*, 291.

(18) Chen, L.; Horiuchi, T.; Mori, T.; Maeda, K. *J. Phys. Chem. B* **1999**, *103*, 1216.

(19) Ito, K.; Yagi, Y.; Hirano, S.; Miyayama, M.; Kudo, T.; Kishimoto, A.; Ujihira, Y. *J. Ceram. Soc. Jpn.* **1999**, *107*, 123.

(20) Hartmann, M.; Bischof, C. *J. Phys. Chem. B* **1999**, *103*, 6230.

(21) Park, D. H.; Park, S. S.; Choe, S. J. *Bull. Korean Chem. Soc.* **1999**, *20*, 715.

(22) Carlsson, A.; Kaneda, M.; Sakamoto, Y.; Terasaki, O.; Ryoo, R.; Joo, S. H. *J. Electron Microsc.* **1999**, *48*, 795.

(23) Ryoo, R.; Joo, S. H.; Jun, S. *J. Phys. Chem. B* **1999**, *103*, 7743.

(24) Lee, J.; Yoon, S.; Hyeon, T.; Oh, S. M.; Kim, K. B. *Chem. Commun.* **1999**, 2177.

(25) Thoelen, C.; Van de Walle, K.; Vankelecom, I. F. J.; Jacobs, P. A. *Chem. Commun.* **1999**, 1841.

(26) Yan, X. W.; Chen, H. Y.; Li, Q. Z. *Acta Chim. Sin.* **1998**, *56*, 1214.

(27) Sing, K. S. W.; Everett, D. H.; Haul, R. A. W.; Moscou, L.; Pierotti, R. A.; Rouquerol, J.; Siemieniowska, T. *Pure Appl. Chem.* **1985**, *57*, 603.

(28) Kruk, M.; Jaroniec, M.; Ryoo, R.; Kim, J. M. *Microporous Mater.* **1997**, *12*, 93.

(29) Jaroniec, M.; Kruk, M.; Olivier, J. P. *Langmuir* **1999**, *15*, 5410.

(30) Kruk, M.; Antochshuk, V.; Jaroniec, M.; Sayari, A. *J. Phys. Chem. B* **1999**, *103*, 10670.

(31) Barrett, E. P.; Joyner, L. G.; Halenda, P. P. *J. Am. Chem. Soc.* **1951**, *73*, 373.

(32) Kruk, M.; Jaroniec, M.; Sayari, A. *Langmuir* **1997**, *13*, 6267.

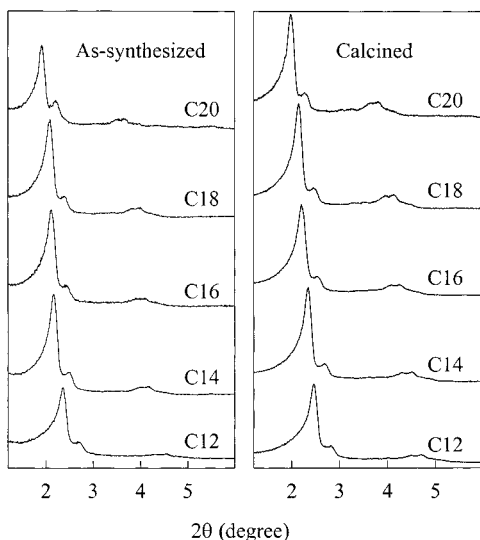


**Figure 1.** Powder X-ray diffraction patterns for MCM-48-U and -C samples.

**Table 1. Properties of MCM-48-U Samples<sup>a</sup>**

sample	$d_{211}$ (nm)	$S_{\text{BET}}$ ( $\text{m}^2 \text{g}^{-1}$ )	$V_t$ ( $\text{cm}^3 \text{g}^{-1}$ )	TGA residue (%)
C20-U	4.62	17	0.10	40
C18-U	4.22	21	0.06	46
C16-U	4.16	28	0.08	49
C14-U	3.94	30	0.06	51
C12-U	3.74	42	0.16	53

<sup>a</sup> Abbreviations:  $d_{211}$ , XRD (211) interplanar spacing;  $S_{\text{BET}}$ , BET specific surface area;  $V_t$ , total pore volume; TGA residue, TGA residue at 1260 K.

## Results and Discussion

**As-Synthesized MCM-48.** Powder X-ray diffraction. MCM-48-U samples had XRD patterns characteristic of well-ordered materials (Figure 1) and exhibited a wide range of unit-cell sizes (see values of the  $d_{211}$  interplanar spacing provided in Table 1; to compare with some of the data reported in the literature, the unit-cell parameters can be calculated as  $6^{1/2} d_{211}$ ). The XRD patterns did not feature any additional reflections, which would indicate contamination of the materials with some ordered mesostructured impurities. These results are quite remarkable for a number of reasons. First, the successful syntheses of MCM-48 templated by alkylammonium surfactants other than cetyltrimethylammonium ( $\text{C}_{16}\text{TMA}^+$ ) have only rarely been reported. A feasibility of MCM-48 synthesis using dodecyltrimethylammonium was mentioned by Stucky et al.,<sup>33</sup> and details of the synthesis were recently reported by Ryoo et al.<sup>6</sup> Synthesis of tetradecyltrimethylammonium-templated MCM-48 was reported in only a few studies,<sup>5,6,33,34</sup> whereas the applicability of octadecyltrimethylammonium was demonstrated only recently.<sup>6</sup> To our best knowledge, a successful synthesis of MCM-48 using eicosyltrimethylammonium ( $\text{C}_{20}\text{TMA}^+$ ) has never been reported before. It should be noted that other surfactants or surfactant mixtures were found suitable for the MCM-48 synthesis, including cetylbenzylid-

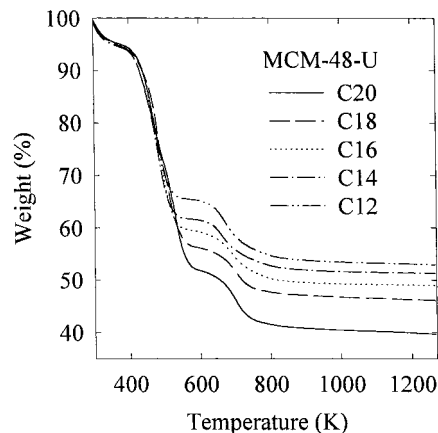


**Figure 2.** Weight change curves for MCM-48-U samples.

methylammonium and gemini alkylammonium surfactants,<sup>3</sup> mixed  $\text{C}_{16}\text{TMA}^+$ /carboxylate anionic surfactants<sup>12,35</sup> and mixed  $\text{C}_{16}\text{TMA}^+$ /dodecylamine surfactants.<sup>6,26</sup>

The  $\text{C}_{20}\text{TMA}^+$ -templated sample belongs to MCM-48 samples with the largest unit-cell size reported so far. Its (211) interplanar spacing is comparable to those of pure MCM-48 samples synthesized by Corma et al. using a procedure involving the high-temperature pore size enlargement of  $\text{C}_{16}\text{TMA}^+$ -templated materials.<sup>36</sup> In the study of Corma et al., MCM-48 samples of even larger unit-cell sizes were also prepared but were found to be contaminated with a lamellar phase because of the partial phase transformation. Similar to the synthesis approach employed in the current study, the synthesis of Corma et al. allows one to prepare MCM-48 with a wide range of unit-cell parameters. This is achieved using a convenient surfactant template ( $\text{C}_{16}\text{TMA}^+$ ) simply by changing temperature and time of the synthesis. However, because of the possibility of contamination with the lamellar phase<sup>36</sup> and the necessity of partial ion exchange of  $\text{C}_{16}\text{TMA}^+$  to the hydroxide form, the method proposed herein may actually be more convenient for preparation of MCM-48 with a wide range of unit-cell dimensions, especially as remarkably high yields of pure-phase products are obtained, as reported before.<sup>6</sup>

**Thermogravimetry.** Thermogravimetric weight change curves for MCM-48-U samples are shown in Figure 2. Three major weight loss regions can be observed. Weight loss below 400 K (~5%) can be attributed to thermodesorption of physically adsorbed water.<sup>37,38</sup> A prominent weight loss at temperatures between 400 and 600 K can be attributed mostly to the decomposition and/or thermodesorption of alkyltrimethylammonium surfactant<sup>1,38</sup> and was actually found to increase as the alkyl chain length, and consequently, the molecular weight, of the surfactant increased (see Figure 2). The weight loss observed between 600 and 800 K appears too large to be attributable solely to the release of water via condensation of silanols.<sup>37,39</sup> However, since mesoporous

(35) Chen, F.; Huang, L.; Li, Q. *Chem. Mater.* **1997**, *9*, 2685.

(36) Corma, A.; Kan, Q.; Rey, F. *Chem. Commun.* **1998**, 579.

(37) Chen, C.-Y.; Li, H.-X.; Davis, M. E. *Microporous Mater.* **1993**, *2*, 17.

(38) Romero, A. A.; Alba, M. D.; Klinowski, J. *J. Phys. Chem. B* **1998**, *102*, 123.

(39) Kruk, M.; Sayari, A.; Jaroniec, M. *Stud. Surf. Sci. Catal.* **2000**, *129*, 567.

(33) Stucky, G. D.; Monnier, A.; Schuth, F.; Huo, Q.; Margolese, D.; Kumar, D.; Krishnamurty, M.; Petroff, P.; Firouzi, A.; Janicke, M.; Chmelka, B. F. *Mol. Cryst. Liq. Cryst.* **1994**, *240*, 187.

(34) Behrens, P.; Glaue, A.; Haggemuller, C.; Schechner, G. *Solid State Ionics* **1997**, *101–103*, 255.

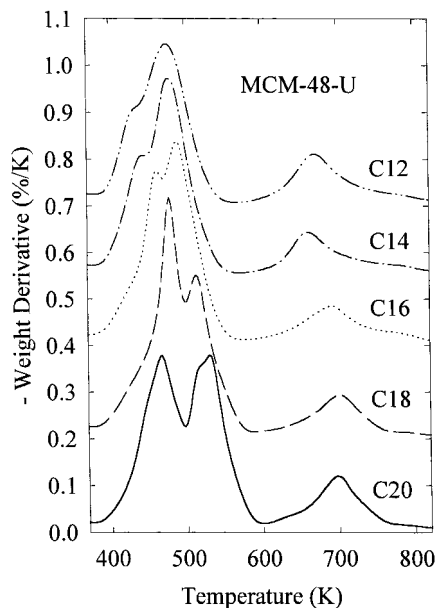


**Figure 3.** Weight change derivatives for MCM-48-U samples. To allow for a better comparison, the data for C18-U, C16-U, C14-U, and C12-U were shifted by 0.2, 0.4, 0.55, and 0.7%/K, respectively.

silicas templated by an oligomeric ethylene oxide surfactant Triton X-100 (one of the cosurfactants used in our study and structurally similar to the other ones applied) were reported to exhibit a major weight loss event at about 700 K,<sup>40</sup> one can assign the weight losses observed between 600 and 800 K for the MCM-48 samples primarily to decomposition and thermodesorption of the oligomeric cosurfactant. Such an assignment is also supported by the fact that the relative magnitude of weight losses at 400–600 K and 600–800 K can be related to the composition of the template mixture used for the synthesis. Namely, the weight loss at 600–800 K was relatively more pronounced when shorter-chain alkyltrimethylammonium surfactant was used and the ionic surfactant/cosurfactant molar ratio was smaller. This also provides an evidence that the ionic surfactant/cosurfactant molar ratio in MCM-48-U was similar to that in the synthesis mixture.

To facilitate further comparison, weight change derivatives (Figure 3) were calculated from the weight change curves (Figure 2). The decomposition/desorption of the ionic surfactant and the nonionic cosurfactant gave rise to pronounced peaks at 400–600 K and about 700 K, respectively, on the weight change derivatives. One may expect that a higher molecular weight ionic surfactant would thermodesorb at higher temperature. There is some evidence of such a behavior, since the position of the peak or peaks corresponding to the loss of the ionic surfactant shifted to some extent to higher temperature as the surfactant chain length increased. However, the overall weight loss behavior was more complicated, which may be related to the fact that the thermodesorption of alkyltrimethylammonium is preceded by its decomposition via Hoffmann elimination.<sup>1</sup> Thus, the temperature of thermodesorption of alkyltrimethylammonium is likely to be governed by its decom-

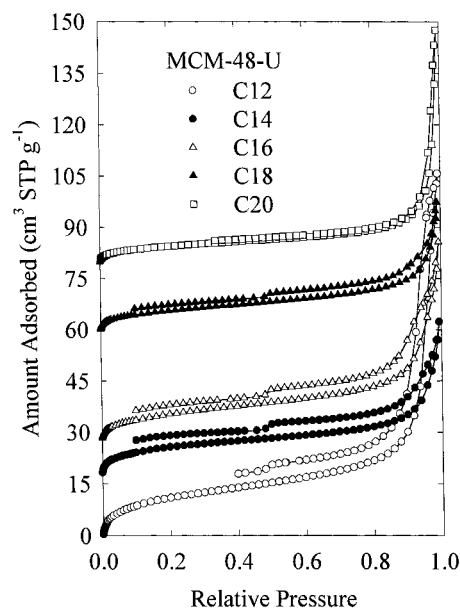


**Figure 4.** Nitrogen adsorption isotherms for MCM-48-U samples. To allow for a better comparison, the data for C14-U, C16-U, C18-U, and C20-U were shifted by 18, 28, 60, and 80 cm<sup>3</sup> STP g<sup>-1</sup>, respectively.

position temperature and the temperature of thermodesorption of the decomposition products (trimethylamine and alkene), and not simply by the molecular weight of the ionic surfactant template.

**Nitrogen Adsorption.** Shown in Figure 4 are nitrogen adsorption isotherms for MCM-48-U samples. The latter exhibited low BET specific surface areas (see Table 1) and their adsorption isotherms did not feature steps of capillary condensation in primary mesopores, which are a prominent feature of adsorption isotherms of calcined MCM-48, as will be discussed later. This clearly demonstrates that the primary mesopores of as-synthesized MCM-48 samples were filled with the surfactant template and thus essentially inaccessible to nitrogen adsorbate. Furthermore, the inaccessibility of these pores provided evidence that the water washing did not remove any appreciable amount of the surfactant from the MCM-48 channels. The inaccessibility of the primary mesopores after the water washing is in contrast to the recently reported results of ethanol washing at room temperature for uncalcined MCM-41, which indicated accessibility of a small fraction of primary mesopores and thus a partial removal of the surfactant from the silica pores.<sup>41</sup> Therefore, samples of as-prepared ordered mesoporous materials used for estimation of the silica/surfactant ratio should be washed with water rather than ethanol.

The amount adsorbed for MCM-48-U samples rapidly increased at relative pressures close to the saturation vapor pressure, which indicated the presence of secondary, presumably interparticular, pores of the size on the borderline between the mesopore and macropore ranges (about 50 nm). The volumes of these pores were determined from the amount adsorbed at a relative pressure of 0.99 and are listed in Table 1. However, because of the lack of the limiting amount adsorbed as the satura-

(40) Sierra, L.; Lopez, B.; Gil, H.; Guth, J.-L. *Adv. Mater.* **1999**, *11*, 307.

(41) Kruk, M.; Jaroniec, M.; Sakamoto, Y.; Terasaki, O.; Ryoo, R.; Ko, C. H. *J. Phys. Chem. B* **2000**, *104*, 292.

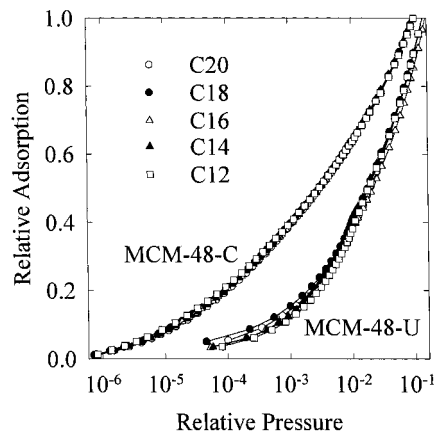


**Figure 5.** Comparison of relative adsorption curves for MCM-48-U and -C samples.

tion vapor pressure was approached, these estimates may be quite inaccurate.<sup>27</sup>

Shown in Figure 5 are low-pressure relative adsorption curves (amounts adsorbed divided by the BET monolayer capacity) for MCM-48-U samples. In contrast to the adsorption behavior of the calcined MCM-48 samples, all the as-synthesized samples adsorbed only small amounts of nitrogen in the low-pressure range, which indicates weak nitrogen–surface interactions and was reported, for instance, for alkylsilyl-modified silicas, including modified MCM-41.<sup>42</sup> The  $\alpha_s$  plot analysis additionally confirmed that low-pressure adsorption properties of MCM-48-U are much closer to those of highly hydrophobic octyldimethylsilyl-modified silicas than to those of bare silicas. Nitrogen–surface interactions similarly weak as those observed here for MCM-48-U were already reported for uncalcined ethanol-washed MCM-41 samples,<sup>41</sup> as well as for uncalcined water-washed MCM-41<sup>43,44</sup> and lamellar phase.<sup>43</sup> This behavior was explained as a result of coverage of the external surface of ordered silicate–surfactant materials with a relatively dense layer of electrostatically bonded alkylammonium surfactant ions with alkyl chains pointing to the exterior of the particles.<sup>41</sup> This behavior was postulated to be a common feature of silicate–surfactant materials whose self-assembly is based on direct ionic interactions.<sup>41</sup> The high-pressure nitrogen adsorption behavior of MCM-48-U confirms the presence of surfactant molecules on the external surface, since the hysteresis loops on adsorption isotherms did not close at relative pressures of about 0.4, that is low-pressure hysteresis was observed (see Figure 4).<sup>27</sup> Such a behavior was commonly observed for silicas modified via chemical bonding of alkylsilanes with long alkyl chains, such as octyl,<sup>42</sup> but is uncommon for siliceous ordered mesoporous materials, for which it was reported so far mainly for MCM-41 with highly degraded, and thus very nonuniform, porous structure.<sup>45</sup> Although nitrogen may possibly penetrate to some extent the surfactant-filled channels of MCM-48, this behavior is highly unlikely

(42) Jaroniec, C. P.; Kruk, M.; Jaroniec, M.; Sayari, A. *J. Phys. Chem. B* **1998**, *102*, 5503.

(43) Kruk, M.; Jaroniec, M.; Yang, Y.; Sayari, A. *J. Phys. Chem. B* **2000**, *104*, 1581.

(44) Jaroniec, M.; Kruk, M.; Sayari, A. *Stud. Surf. Sci. Catal.* **2000**, *129*, 587.

(45) Sayari, A.; Liu, P.; Kruk, M.; Jaroniec, M. *Chem. Mater.* **1997**, *9*, 2499.

**Table 2. Properties of MCM-48-C Samples<sup>a</sup>**

sample	$d_{211}$ (nm)	$S_{\text{BET}}$ ( $\text{m}^2 \text{g}^{-1}$ )	$V_t$ ( $\text{cm}^3 \text{g}^{-1}$ )	$V_p$ ( $\text{cm}^3 \text{g}^{-1}$ )	$S_{\text{ex}}$ ( $\text{m}^2 \text{g}^{-1}$ )	$w_{\text{KJS}}$ (nm)
C20-C	4.46	1130	1.46	1.14	110	4.53
C18-C	4.11	1150	1.25	1.07	90	4.12
C16-C	3.99	1110	1.18	0.95	120	3.93
C14-C	3.76	1100	1.04	0.90	60	3.68
C12-C	3.59	1060	1.09	0.78	110	3.49

<sup>a</sup> Abbreviations:  $S_{\text{ex}}$ , external surface area;  $w_{\text{KJS}}$ , primary mesopore size. For other notation, see Table 1.

**Table 3. Properties of MCM-48-EA Samples<sup>a</sup>**

sample	$d_{211}$ (nm)	$S_{\text{BET}}$ ( $\text{m}^2 \text{g}^{-1}$ )	$V_t$ ( $\text{cm}^3 \text{g}^{-1}$ )	$V_p$ ( $\text{cm}^3 \text{g}^{-1}$ )	$S_{\text{ex}}$ ( $\text{m}^2 \text{g}^{-1}$ )	$w_{\text{KJS}}$ (nm)
C20-EA	4.57	1020	1.29	1.07	110	4.59
C18-EA	4.24	1180	1.32	1.14	100	4.18
C16-EA	4.14	1060	1.19	0.98	90	4.05
C14-EA	3.91	1110	1.11	0.95	90	3.77
C12-EA	3.82	1010	1.07	0.79	70	3.57

<sup>a</sup> For notation, see Tables 1 and 2.

for MCM-48-U samples since in this case the differences between the amount adsorbed on the adsorption and desorption branches at the same pressure below the relative pressure of 0.4 would probably increase as the percentage of the surfactant in the samples increased. These differences were actually found to decrease as the amount of the template increased, but they increased as the specific surface area increased. Thus, the low-pressure hysteresis observed is most likely attributable to the peculiarities of nitrogen interactions with long alkyl chains of the surfactant bonded to the external surface of as-synthesized MCM-48.

**Calcined MCM-48. Powder X-ray Diffraction.** XRD spectra for the calcined samples were characteristic of well-ordered MCM-48 (Figure 1). In all cases, the shrinkage upon calcination was relatively small (below 5%, see  $d_{211}$  interplanar spacing values in Tables 1 and 2). The unit-cell size for C20-C is comparable to the highest reported in the literature for calcined phase-pure MCM-48.<sup>36</sup>

**Nitrogen Adsorption.** Nitrogen adsorption isotherms for MCM-48-C silicas are shown in Figure 6. They exhibited sharp capillary condensation steps<sup>46–48</sup> centered at relative pressures between 0.30 and 0.45, which indicated that the average pore sizes of these samples covered a wide range of values. Such a behavior has been reported for MCM-41 prepared using alkylammonium surfactants of different alkyl chain length.<sup>41,49,50</sup> In the case of C16-C, C18-C, and C20-C MCM-48, the positions of the capillary condensation steps were quite similar to those for MCM-41 synthesized using surfactants with the same alkyl chain lengths. However, in the case of C14-C and C12-C MCM-48, the capillary condensation steps were observed at relative pressures

(46) Vartuli, J. C.; Schmitt, K. D.; Kresge, C. T.; Roth, W. J.; Leonowicz, M. E.; McCullen, S. B.; Hellring, S. D.; Beck, J. S.; Schlenker, J. L.; Olson, D. H.; Sheppard, E. W. *Chem. Mater.* **1994**, *6*, 2317.

(47) Schmidt, R.; Stocker, M.; Ellestad, O. H. *Stud. Surf. Sci. Catal.* **1995**, *97*, 149.

(48) Sayari, A.; Danumah, C.; Liu, P.; Jaroniec, M. In *Characterization of Porous Solids IV*; McEnaney, B., Mays, T. J., Rouquerol, J., Rodriguez-Reinoso, F., Sing, K. S. W., Unger, K. K., Eds.; Royal Society of Chemistry: Cambridge, 1997; p 557.

(49) Kruk, M.; Jaroniec, M.; Sayari, A. *J. Phys. Chem. B* **1997**, *101*, 583.

(50) Sonwane, C. G.; Bhatia, S. K. *Chem. Eng. Sci.* **1998**, *53*, 3143.

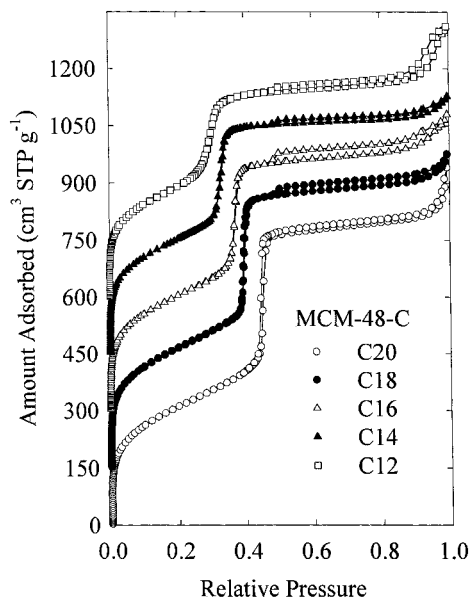


**Figure 6.** Nitrogen adsorption isotherms for MCM-48-C samples. To allow for a better comparison, data for C18-C, C16-C, C14-C and C12-C were shifted by 150, 300, 450, and 600  $\text{cm}^3 \text{STP g}^{-1}$ , respectively.

higher than those for MCM-41 samples prepared using the corresponding alkylammonium surfactants. This may be related to the use of cosurfactants in the MCM-48 synthesis, especially as calcined MCM-48 samples prepared under similar conditions without the application of cosurfactants exhibited capillary condensation at somewhat lower pressures.<sup>5</sup> The latter observation also suggests that the addition of neutral cosurfactant used increases the diameter of the alkyltrimethylammonium micelles in the silicate-surfactant structure. It is also interesting to note that the relative pressure of capillary condensation for C20-C is comparable to the highest reported in the literature for both phase-pure and lamellar-phase-contaminated MCM-48.<sup>36</sup> Since capillary condensation pressure in general increases as the pore diameter increases,<sup>27,32</sup> one can conclude that the pore size of C20-C is among the highest MCM-48 pore sizes reported to date.<sup>36</sup>

In the case of C20-C, the capillary condensation was clearly accompanied by adsorption-desorption hysteresis, which is expected to be observed at relative pressures above about 0.4 in the case of nitrogen adsorption at 77 K.<sup>27,32</sup> Some evidence of adsorption-desorption hysteresis was also observed for other samples, primarily for C18-C and C16-C, and to lower extent for C14-C and C12-C, but since the width of these hysteresis loops was very small, probably within experimental error for C14-C and C12-C, the capillary condensation behavior of these samples can be considered as essentially reversible, especially in the case of C14-C and C12-C. The adsorption isotherms for MCM-48-C samples exhibited hysteresis loops at relative pressures of about 0.5, which can be attributed to the presence of secondary pores. The similarity of the hysteresis loops of the as-synthesized and calcined samples (see Figures 4 and 6) indicates that the secondary porosity formed during the hydrothermal synthesis and thus is likely to be a feature of the material's particles. Further, this behavior indicates that it is highly improbable that any appreciable parts of the

silicate framework collapsed during calcination, since this would lead to development of some new secondary pores not observed for the as-synthesized samples. There was no evidence of such a behavior for the MCM-48 samples, although such a behavior was reported for MCM-41 contaminated with a lamellar phase.<sup>43</sup>

Low-pressure adsorption properties of MCM-48-C samples were found to be highly similar to one another (see Figure 5) and to those previously reported for ordered and conventional mesoporous silicas.<sup>5,28,29,32,41,48</sup> This similarity was additionally confirmed by an excellent linearity of initial parts of  $\alpha_s$  plots for MCM-48-C samples, when the silica reference adsorbent was used.

The selected structural properties of MCM-48-C samples are listed in Table 2. The materials exhibited similar BET specific surface areas of about  $1100 \text{ m}^2 \text{ g}^{-1}$  and their primary mesopore volumes systematically increased as the alkyltrimethylammonium surfactant chain length increased, similar to the properties of MCM-41.<sup>41,49,50</sup> The primary mesopore volume of MCM-48-C was clearly correlated with the percentage of the template in MCM-48-U, which can be estimated from TGA as the weight loss between  $\sim 400$  and  $800 \text{ K}$  (see Figure 2 and Table 2). The external surface area of MCM-48-C samples was found to be much larger than the specific surface area (that is external surface area of particles) of MCM-48-U samples. The increase in the external surface area upon calcination was often too large to result from the surfactant removal. This may be attributable to the effect of presence of the surfactant ions on the external surface of MCM-48-U particles, since the long alkyl chains are capable of adopting different conformations and thus may smooth out imperfections or roughness of the external silicate surface. Alternatively, the calcination might cause structural degradation of a small part of the material, major damage being highly unlikely on the basis of the other data discussed above. Another possibility is that some amount of the ionic surfactant, which was not electrostatically bonded to the silicate framework, and/or some amount of cosurfactant were left on the surface of particles of MCM-48-U despite the water washing. This might have led to smoothing of the surface roughness of the as-synthesized material. However, similar relation between the surface areas of surfactant-containing and calcined samples was observed for MCM-41 samples.<sup>41</sup> In this case, the as-prepared samples were subjected to ethanol washing and there was evidence that such washing led to removal of essentially all surfactant, which was not bonded strongly to the silicate framework. This suggests that the possible influence of unwashed template on the external surface area changes observed for the MCM-48 samples is likely to be small.

As can be seen in Figure 7, MCM-48-C samples exhibited narrow pore size distributions, especially in the case of C16-C, C18-C, and C20-C, and average pore sizes systematically covering the range from 3.5 to 4.5 nm (see Table 2). If the MCM-48 samples of lower pore size are required for some purposes, they can be prepared without use of neutral cosurfactants, for instance using the method described in ref 5. It should be noted that the accuracy of the pore size determination method employed herein<sup>32</sup> is based on calibration using MCM-41 silicas. Since the latter have a somewhat

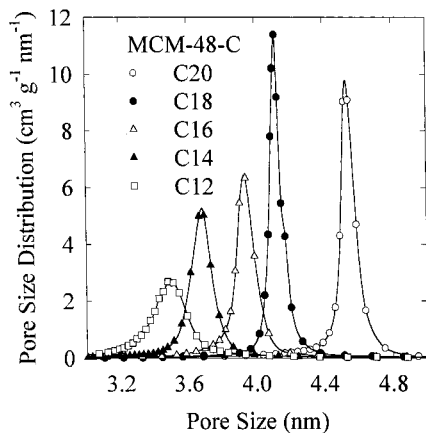


**Figure 7.** Pore size distributions for MCM-48-C samples.

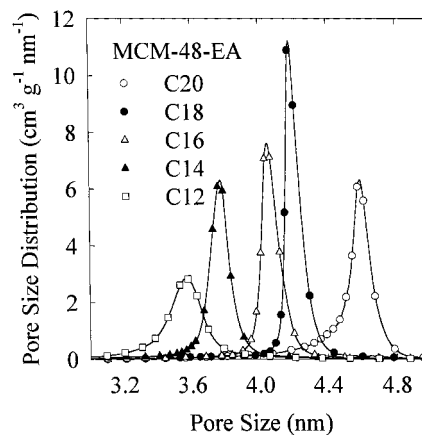


**Figure 9.** Pore size distributions for MCM-48-EA samples.

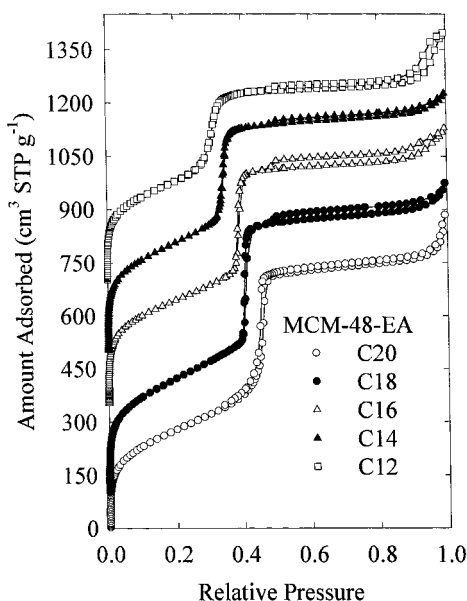


**Figure 8.** Nitrogen adsorption isotherms for MCM-48-EA samples. To allow for a better comparison, data for C18-EA, C16-EA, C14-EA, and C12-EA were shifted by 150, 300, 450, and 600 cm<sup>3</sup> STP g<sup>-1</sup>, respectively.

different pore geometry than MCM-48, the method used may produce some systematic errors in the case of MCM-48.

**Ethanol/HCl Washed MCM-48.** Powder X-ray Diffraction. MCM-48-EA samples exhibited XRD patterns similar to those shown in Figure 1 for the corresponding as-synthesized and calcined samples. There was no evidence of any appreciable unit-cell size change upon ethanol/HCl washing.

**Nitrogen Adsorption.** Nitrogen adsorption isotherms for MCM-48-EA samples (Figure 8) were similar to those of the calcined samples. The BET specific surface areas of the corresponding MCM-48-EA and MCM-48-C samples were in most cases similar and the pore volumes as well as primary mesopore sizes of the former were usually larger. The pore size differences can be attributed to the fact that the MCM-48 samples shrank upon calcination, but did not shrink upon surfactant removal via solvent extraction. The width of the pore size distributions was also found to be similar for the samples prepared using these two methods of surfactant removal (see Figures 7 and 9). C20 MCM-48 exhibited somewhat different behavior, since the BET specific

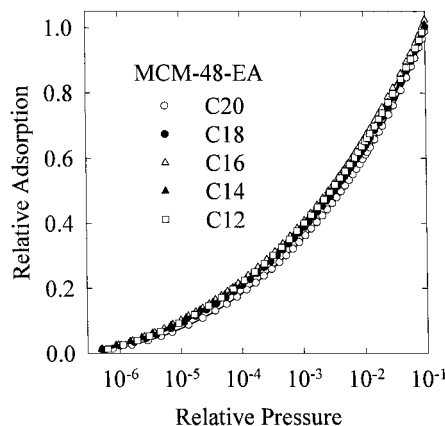


**Figure 10.** Relative adsorption curves for MCM-48-EA samples.

surface area, primary mesopore volume and total pore volume of C20-EA were noticeably lower than those of C20-C, which also exhibited a much more narrow pore size distribution. The data discussed above indicate that the template was successfully removed via the ethanol/HCl washing, except for the C20-EA, for which a retention of a certain amount of the template in the pores was a distinct possibility. To verify this, the low-pressure parts of the relative adsorption curves for MCM-48-EA samples were compared. They were generally similar to one another (Figure 10) and to those of the calcined samples (see Figure 5). However, the low-pressure relative adsorption was found to be somewhat lower for C20-EA than for the other MCM-48-EA samples. Since it was already demonstrated that the presence of surfactant on the silicate surface significantly reduces low-pressure nitrogen adsorption, the behavior of C20-EA is indicative of the retention of a small amount of surfactant. Probably, the C<sub>20</sub>TMA<sup>+</sup> cationic surfactant is difficult to wash completely using the ethanol/HCl mixture because of the increasing hydrophobicity of the surfactant as its alkyl chain length increases.

**Thermogravimetry.** MCM-48-C samples were found to exhibit the weight loss of about 1% in the temperature range from 400 to 800 K, which can be attributed to condensation of silanols.<sup>37</sup> Since ethanol/HCl washed samples have a lower degree of silanol condensation than the calcined samples,<sup>37</sup> the former are expected to exhibit at least 1% weight loss in this temperature range. MCM-48-EA samples actually exhibited weight

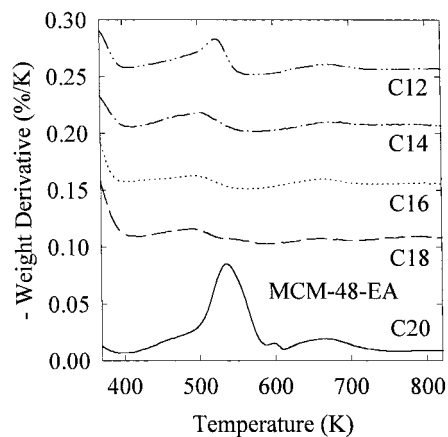


**Figure 11.** Weight change derivatives for MCM-48-EA samples. To allow for a better comparison, the data for C18-EA, C16-EA, C14-EA, and C12-EA were shifted by 0.1, 0.15, 0.2, and 0.25%/K, respectively.

loss between 3 and 4.5%, except for C20-EA, which exhibited the weight loss as high as 9% between 400 and 800 K. These results suggest that the amount of surfactant remaining in the MCM-48-EA samples was below 8% for C20-EA and below 2–3.5% for the other MCM-48-EA samples. As can be seen in Figure 11, C20-EA was the only sample, which exhibited a strong peak on the weight change derivative in the temperature range of surfactant decomposition/desorption. This correlates well with the conclusions from nitrogen adsorption data analysis and confirms its quite remarkable capability of monitoring surfactant removal and detection of surfactant present in the amounts as small as 10%. The weight loss derivative for C12-EA also provided some evidence for a small amount of the template in the structure, but since this amount is below 3.5% as discussed above, it is not easy to detect it from gas adsorption data. It is also interesting that in the case of C20-EA, a pronounced peak on the weight loss derivative was observed in the region of the ionic surfactant decomposition/desorption, but the peak corresponding to removal of the cosurfactant at higher temperature (about 700 K) was weak. This indicates that the washing led to a much more quantitative removal of the neutral cosurfactant in comparison to the ionic surfactant, which is not unexpected since the latter is covalently bonded to the silicate framework, whereas the former is likely to exhibit much weaker interactions with the framework and thus, to be extracted more

readily. For instance, nonionic surfactants analogous to those used in this work as cosurfactants can be extracted from the templated silicas using ethanol.<sup>51</sup>

## Conclusions

The current study demonstrated that the recently reported synthesis of MCM-48 using mixtures of alkyltrimethylammonium surfactants and nonionic cosurfactants is capable of providing highly ordered samples with a wide range of average pore sizes and unit-cell sizes. In particular, it is possible to synthesize large-pore MCM-48 using eicosyltrimethylammonium. Application of characterization methods based on XRD, nitrogen adsorption, and thermogravimetry allows one to obtain important insights into the structure of MCM-48. XRD allowed us to demonstrate that the obtained MCM-48 materials were not contaminated by any periodic surfactant–silicate impurities, which commonly form during MCM-48 preparation using other synthesis procedures. Nitrogen adsorption was used to evaluate the pore size, pore volume, and BET specific surface area, but since this technique is capable of discriminating between surface properties of materials, it also allowed us to detect the presence of surfactant ions on the external surface of particles of as-synthesized MCM-48 and to monitor effectiveness of surfactant removal via solvent extraction. TGA was also found to be highly useful for the latter purpose, and allowed us to determine the surfactant content in the samples and to demonstrate that both the cationic surfactant and cosurfactant are incorporated in the micelles of the as-synthesized MCM-48 materials. Finally, the combined XRD, nitrogen adsorption and TGA analysis was used to demonstrate that the secondary porosity of calcined MCM-48 is determined primarily at the stage of the hydrothermal synthesis and that an appreciable partial structural collapse of the silicate framework upon calcination was highly unlikely.

**Acknowledgment.** The donors of the Petroleum Research Fund administered by the American Chemical Society are gratefully acknowledged for a partial support of this research.

CM990764H

(51) Bagshaw, S. A.; Prouzet, E.; Pinnavaia, T. J. *Science* **1995**, *269*, 1242.